

Interactive process of separation bubble and large-scale vortical structure: FPGA-DMD approach for Phase-locking PIV measurement

Yifan Deng¹², Peng Wang¹², Hao Fu¹², Yingzheng Liu^{12*}

¹Shanghai Jiao Tong University, Key Laboratory of Education Ministry for Power Machinery and Engineering, School of Mechanical Engineering, Shanghai, China

²Shanghai Jiao Tong University, Gas Turbine Research Institute, Shanghai, China

* yzliu@sjtu.edu.cn

Abstract

Unsteady behaviors of the separated and reattaching flows are spatio-temporally interacted in the limited spatial extent, while their different temporal/spatial scales and different dynamic statuses would introduce considerable complexity into the interactive process. An improved phase determination rule, which follows the phase-match relationship of individual events and their temporal relation faithfully, was adapted to elucidate the complex interactive process of the flapping separation bubble and the shedding large-scale vortical structures. It takes full advantage of the DMD analysis, which performing on the wall-pressure fluctuations measured by the arrayed microphone to determine the phase match relationship between a period of the flapping separation bubble and three consecutive periods of the shedding vortical structures. Using the FPGA configuration to generate the conditional signal firing the low-sampling-rate high-spatio-resolution PIV setup, a close-up view of the strong interaction processes between the separation bubble and the large-scale vortical structures was distinctly revealed. Sixteen successive phase-averaged flow fields around a finite blunt plate with a length-to-height-ratio $L/D = 6$ were accurately determined with a mainstream Reynolds number of $Re_{in} = 1.58 \times 10^4$. Then, leveraging the velocity fields, the global pressure fields have been reconstructed to demonstrate the motivation behind the unsteady separated and reattaching flow phenomenon. Finally, the three interactive events were divided into two distinct modes named as explosion mode and developing mode, which were compared with the quantitative analysis. In continuation of the previous study by Deng et al. (2019), this study, using the improved phase determination rule based on the proposed FPGA-DMD approach, demonstrated the interactive process of the flapping separation bubble and the shedding large-scale vortical structures clearly.

1 Introduction

The separated and reattaching flow around a finite blunt plate typically occurring in turbine blades, suspension bridges and high-rise building [Nakamura et al. (1991), Mills et al. (2003)], which usually result in troublesome fluid-induced structure vibrations and acoustic emissions [Naudascher et al. (2012)], are characterized by separation bubble, large-scale vortical structures and their interactions. The dominant unsteady flow behaviors occurring at different temporal/spatial scales and with different dynamic statuses bring about complex flow phenomenon above the finite blunt plate and introduces substantial difficulties to figure out the flow mechanism behind the separated and

reattaching flow. Due to the limitation of experimental measurements and analysis methods, it is difficult to capture the individual processes of each unsteady flow events and further understand the interactive effects between them. Therefore, it is essential that with a sophisticated strategy developing a comprehensive understanding of the interactive process between separation bubble and large-scale vortical structures would be highly desirable.

Various efforts have been made to elucidate the mechanism buried in turbulent separated and reattaching flow. Using surface-pressure fluctuations measured by a pointwise pressure transducer as the conditional signal, Kiya et al. (1985) made considerable efforts to survey the velocity variations through hot-wire probes around a finite blunt plate and reproduce the bubble's enlargement-and-shrinkage motion. However, considering the multiple energetic processes superimposed in the turbulent separated and reattaching flow, point measurement at selective placement would be difficult to provide global and accurate message in practice. Arrayed hotwire anemometers of the separated flows around a finite plate ($L/D < 15$) with a sharp trailing edge at low Reynolds numbers by Nakamura et al. (1991) confirmed that vortex shedding over the plate is characterized by impingement-shear-layer instability in which the separated and reattaching shear layer becomes unstable. Considering that the spatiotemporal fluctuations of wall-pressure on the plate surface are directly related to unsteady flow behaviors buried behind the separated and reattaching flow, Zhang et al. (2012) using arrayed microphones measured wall-pressure fluctuations on a plate's surface ($L/D=9$) and identified two unsteady energetic events, i.e., shedding large-scale vortical structures and near-wake vortices. Particle image velocimetry (PIV) measurements of the separated and reattaching turbulent flow over a blunt plate by Mills et al. (2003) and Taylor et al. (2011) obtained the time-averaged velocity and vorticity fields and tried to explain the shedding motion of leading-edge vortex and trailing-edge vortex. Combining a low-sampling-rate PIV setup with a high-sampling-rate microphone array, Zhang et al. (2017) conducted a POD analysis of both velocity field and wall-pressure fluctuations and identified two energetic feature modes reflecting the impinging motion of large-scale vortical structures and the shedding motion of Karman-vortex structures in the wake. Recently, a sophisticated online FPGA-DMD approach [Deng et al. (2019)] for phase-locking PIV measurements was preliminarily applied to investigate the unsteady behaviors of turbulent separated and reattaching flow and successfully extracted the individual evolution process of each energetically unsteady events, i.e., the flapping motion of the separation bubble, the impinging motion of the leading-edge vortex and the shedding motion of the trailing-edge vortex. However, due to the complexity of phenomenon and the limitations of trigger rules, the interactive process of separation bubble and large-scale vortical structures were not demonstrated clearly. Therefore, it is essential to employ an improved phase determination rule, which faithfully followed the relationship of the first and second DMD mode coefficient corresponding to the motion of separation bubble and large-scale vortical structures, to further investigated the flow mechanism behind turbulent separated and reattaching flow.

In continuation of the previous study by Deng et al. (2019), this study focuses on the interactive process of separation bubble and large-scale vortical structures spatially and temporally. Here, through the preliminary analysis of wall-pressure fluctuations, a remarkable rule between separation bubble and large-scale vortical structures was founded. Combined with the fast FPGA-based modal analysis system, the phase information of the interactive process was identified and then a low-sampling-rate PIV setup was fired to record the spatio-temporal evolution of these two flow behaviors. Subsequently, a clear panoramic view of the phase-dependent flow fields determined

using the phase-locking PIV technique, revealing the characteristics and evolution of the interactive process taken place between these two flow events. Then, based on the phase-dependent flow fields a global pressure field was reconstructed to demonstrate the motivation behind the unsteady separated and reattaching flow. Finally, two very different coupling phenomenon occurring between the flapping separation bubble and the impinging leading-edge vortex was selected to compare with each other.

2 Experimental Setup

The experiments was set up in an open-circuit wind tunnel previously used by Liu et al. (2015), and diagrams of the phase-locked PIV setup is presented in Fig. 1. A diffuser and a smooth contraction with a contraction ratio of 6:1 were used to straighten the mainstream airflow, which was driven by a centrifugal blower and a 1.5kW motor. The mainstream channel had a cross section of $300 \times 300 \text{ mm}^2$ and was 2000 mm in length. The average mainstream velocity (U_{in}) was maintained at 10 m/s, resulting in a Reynolds number $Re_{in} = 1.58 \times 10^4$ based on the feature size of the plate.

The wall-pressure fluctuation over the blunt plate in the separated flow was instantaneously measured using arrayed ICP-type 1=400 microphones (G.R.A.S., 40PQ, Denmark). A real-time computation and peak detection method, which was built into a FPGA control system (cRIO-9039, NI, USA), was used to obtain the periodic DMD coefficients and determine the peak values. To ensure that the PIV systems was sampled at almost 1HZ, a TTL signal was rapidly transferred to the PIV synchronizer once the FPGA control system had successively captured enough peak values. Immediately the PIV synchronizer triggered a pulsed Nd:YAG laser with a 135 mJ/pulse (532 nm, 8 ns, Litron, UK) and a high-image-density CCD (4872×3248 pixels) camera (IPX 16M, IMPERX, USA) to capture the phase-averaged flow fields. The high sampling frequency and operating speed of the FPGA control system guaranteed that the error of phase detection was less than 0.2%.

In experiments, the CCD camera recorded 1000 images of the phase-dependent flow field for each phase, and seeding of the measurement region was performed using Di-Ethyl-Hexyl-Sebacat (DEHS) droplets. The standard PIV cross-correlation algorithm, incorporating sub-pixel recognition, sub-region distortion, and window-offset methods, were used to determine the phase-averaged flow fields. The interrogation window size was 32×32 pixels with a 50% overlap, which leading to a measurement grid with a spacing of $1.1\text{mm} \times 1.1\text{mm}$. The error of PIV particle displacement between two images was less than 0.1 pixels, which caused that the uncertainty of the velocity field was less than 2%.

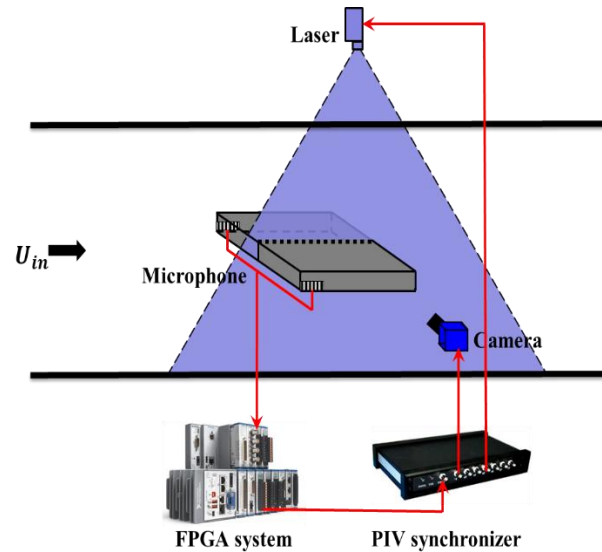


Figure 1: Experimental setup

3 Discussion

A significant characteristic for evaluating the intensity of vortex structures is the vorticity. The spatiotemporal evolution of velocity vector and vorticity contour corresponding to the first interaction process are shown in Fig. 2. The red region represents the shape and intensity of clockwise vortices, and the blue region represents the shape and intensity of counterclockwise vortices. In the phase 0° , due to the existence of separation bubbles, a hairpin zone appears in the front of the plate, and the vorticity increases suddenly. In the flutter region of from phase 0° to phase 180° on a finite blunt plate, the spatial scale of separation bubbles increases and enlarges gradually, making the hairpin region with positive vorticity enlarge continuously. At the same time, due to the shedding motion of large-scale vorticity structure, the elliptical region with positive vorticity drops from $x/D=5.50$ to $x/D=9.00$. As the large-scale eddy structure falls off and expands downstream, the scale of elliptical region increases with the gradual attenuation of strong vorticity. The spatiotemporal evolution of velocity vector and vorticity contour corresponding to the first interaction process are shown in Fig. 3, which had a similar motion corresponding to the first interactive process. In Fig. 4, the spatiotemporal evolutions of the velocity vectors and vorticity contours for the third interactive process between separation bubble and large-scale vortical structures performed a distinct flow behavior.

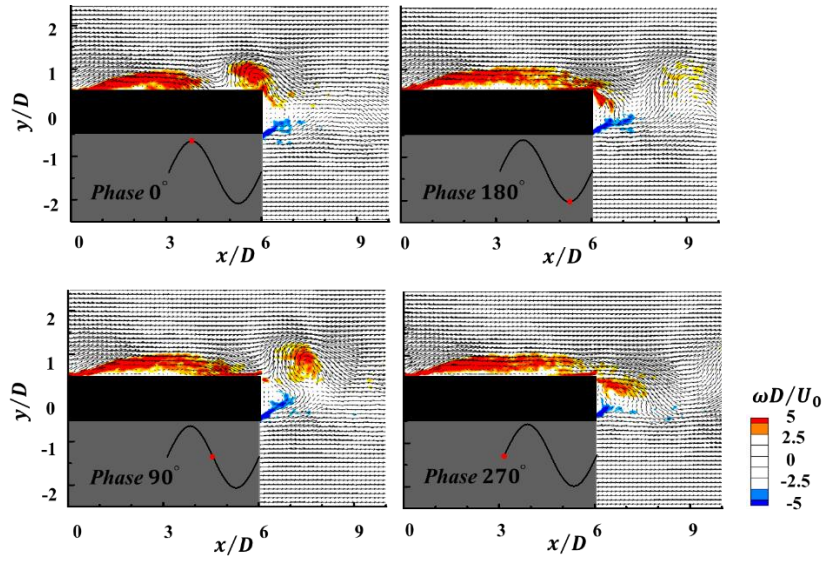


Figure 2: The spatiotemporal evolutions of the velocity vectors and vorticity contours corresponding to the first interactive process

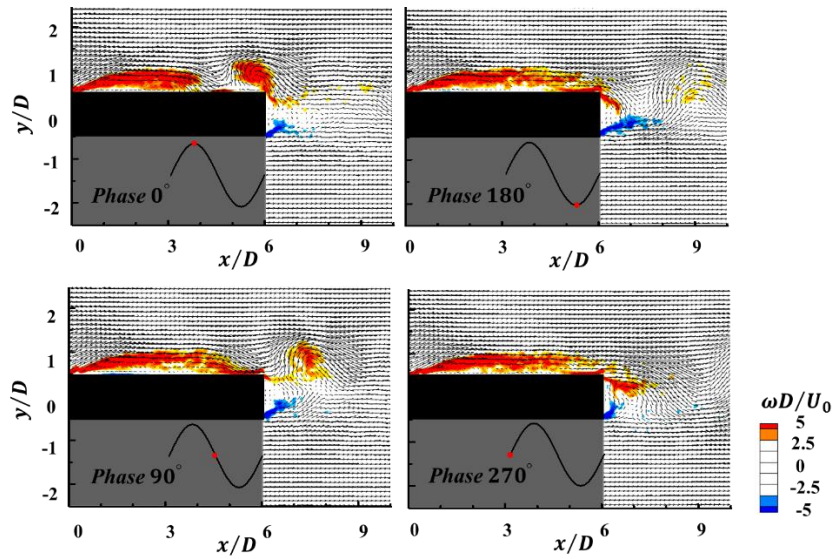


Figure 3: The spatiotemporal evolutions of the velocity vectors and vorticity contours corresponding to the second interactive process

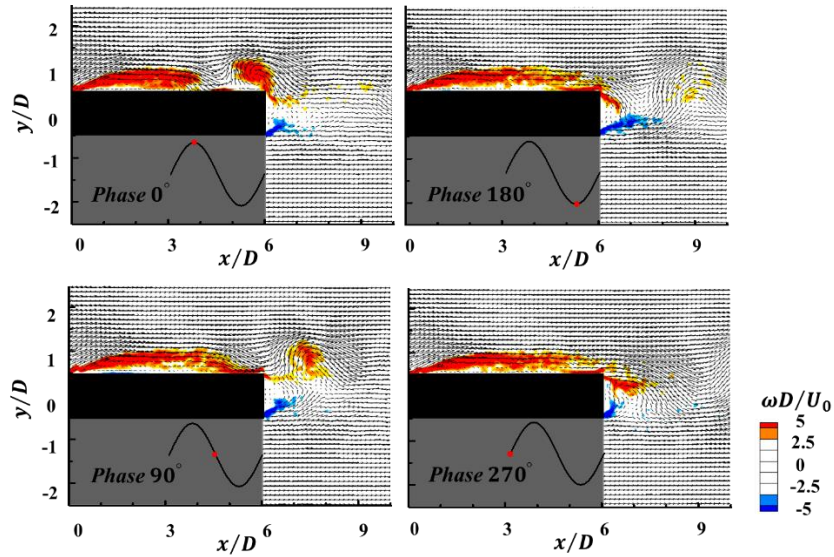


Figure 4: The spatiotemporal evolutions of the velocity vectors and vorticity contours corresponding to the third interactive process

4 Conclusion

In continuation of the previous study by Deng et al. (2019), this study, using the improved phase determination rule based on the proposed FPGA-DMD approach, demonstrated the interactive process of the flapping separation bubble and the shedding large-scale vortical structures clearly. An improved phase determination rule, which follows the phase-match relationship of individual events and their temporal relation faithfully, was adapted to elucidate the complex interactive process of the flapping separation bubble and the shedding large-scale vortical structures. It takes full advantage of the DMD analysis, which performing on the wall-pressure fluctuations measured by the arrayed microphone to determine the phase match relationship between a period of the flapping separation bubble and three consecutive periods of the shedding vortical structures. Using the FPGA configuration to generate the conditional signal firing the low-sampling-rate high-spatio-resolution PIV setup, a close-up view of the strong interaction processes between the separation bubble and the large-scale vortical structures was distinctly revealed. Sixteen successive phase-averaged flow fields around a finite blunt plate with a length-to-height-ratio $L/D = 6$ were accurately determined with a mainstream Reynolds number of $Re_{in} = 1.58 \times 10^4$. Then, leveraging the velocity fields, the global pressure fields have been reconstructed to demonstrated the motivation behind the unsteady separated and reattaching flow phenomenon. Finally, the three interactive events were divided into two distinct modes named as explosion mode and developing mode, which were compared with the quantitative analysis.

Acknowledgements

The authors gratefully acknowledge financial support for this study from the National Natural Science Foundation of China (11802177, 11725209) and the China Postdoctoral Science Foundation (2018M630439).

References

- Kiya M, Sasaki K (1985) Structure of large-scale vortices and unsteady reverse flow in the reattaching zone of a turbulent separation bubble. *J Fluid Mech.* 154:463–491
- Nakamura Y, Ohya Y, Tsuruta H (1991) Experiments on vortex shedding from flat plates with square leading and trailing edges. *J. Fluid Mech.* 222:437–447
- Mills R, Sheridan J, Hourigan K (2003) Particle image velocimetry and visualization of natural and forced flow around rectangular cylinders. *J. Fluid Mech.* 478:299–323
- Taylor Z, Palombi E, Gurka R, Kopp G (2011) Features of the turbulent flow around symmetric elongated bluff bodies. *J. Fluids Struct.* 27:250–265
- Zhang QS, Liu YZ (2012) Wall-pressure fluctuations of separated and reattaching flow over blunt plate with chord-to-thickness ratio $c/d = 9.0$. *Exp Therm Fluid Sci.* 42:125–135
- Naudascher E, Rockwell D (2012) Flow-induced vibrations: An engineering guide 2012. *Dover Publications*
- Liu YZ, Zhang QS (2015) Dynamic mode decomposition of separated flow over a finite blunt plate: Time-resolved particle image velocimetry measurements. *Experiments in Fluids* 56:148
- Zhang QS, Liu YZ (2017) Separated flow over blunt plates with different chord-to-thickness ratios: Unsteady behaviors and wall-pressure fluctuations. *Exp Therm Fluid.* 84:199–216.
- Deng YF, Wang P, Liu YZ (2019) Phase-locking Particle Image Velocimetry Measurement of Unsteady Flow Behaviors: Online Dynamic Mode Decomposition Using Field-programmable Gate Array. *Physics of Fluids* 31:025109